PLA/PCL ecoblends: Effect of PCL addition on the toughness of PLA.

N. León[1,*], O.O. Santana[1,*], M. Hortòs[2], S. Espino[2], M. Ll. Maspoch

[1] Centre Català del Plàstic (CCP), Departament de Ciència i Enginyeria de Materials, Universitat Politècnica de Catalunya, BARCELONATECH, Avda. Eduard Maristany 16, 08019 Barcelona, Spain.
[2] Ercros S.A., Av. Diagonal 595, 08014 Barcelona, España.
[*] Persona de contacto: noel.leon@upc.edu

RESUMEN

El comportamiento a fractura de una "Ecoblend" de Poli(Ácido Láctico) (PLA) con Poli(Caprolactona) (PCL) adecuadamente compatilibilizada ha sido estudiado y comparado con el PLA base. El estudio se llevó a cabo sobre probetas de tipo SENB obtenidas a partir de barras prismáticas (4x10 mm) producidas mediante moldeo por inyección. Para asegurar condiciones ideales de fisura aguda y reproducibilidad de resultados, tras el entallado mecánico se agudizó mediante ablación por láser pulsante en femtosegundos (femtoláser). Aplicando la teoría de mecánica de la fractura elástico lineal, el factor provisional de intensificación de tensiones (K_Q) y el trabajo específico de fractura (w_f) (parámetro alternativo a la resistencia al impacto estandarizada) fueron determinados siguiendo la metodología de monoentalla (a/w=0.45) con 5 réplicas a velocidades de solicitación moderamente altas (1 $m.s^{-1}$, impacto instrumentado en configuración Charpy). La fase PCL promueve un incremento en 1,5 veces en K_Q y de 7 veces en w_f. Las evidencias fractográficas revela que la deformación y la cavitación de la fase PCL promueven el alivio de la triaxialidad local, lo que puede causar un aumento de la tensión hidrostática local necesaria para iniciar las crazes y su posterior ruptura en condiciones de impacto. A a bajas velocidades de solicitación (ensayos de tracción), este proceso de cavitación/fibrilación suprime los fenómenos de crazing de la matriz de PLA favoreciendo su cedencia y deformación plástica.

PALABRAS CLAVE: PLA, PLA/PCL, ecoblends, LEFM, fractura.

ABSTRACT

The fracture behaviour of an "Ecoblend" of Poly(Lactic Acid) (PLA) with Poly(ε-Caprolactone) (PCL) suitably compatibilized has been studied and compared with the base PLA. The study was carried out on SENB-type specimens obtained from prismatic bars (4x10 mm) produced by injection molding. To ensure ideal conditions for acute cracking and reproducibility of results, after mechanical notching, it was sharpened by pulsed laser ablation in femtoseconds (femtolaser). Applying the linear elastic fracture mechanics (LEFM) theory, the provisional stress intensity factor (K_Q) and the specific work of fracture (w_f) (i.e., an alternative parameter to the standardised impact resistance) were determined following the single notch methodology (a/w=0.45) with at least 5 repetitions, using moderately high solicitation rates (1 $m.s^{-1}$, impact instrumented in Charpy configuration). PCL promotes a one-and-a-half-fold stress intensification factor needed to initiate crack propagation and a 7-time increase of energy consumed during the process. Fractographic evidence reveals that the PCL phase deformation and cavitation promote relief of the local triaxiality which can cause an increase of the local hydrostatic stress needed to initiate the crazes and its subsequent rupture in impact conditions. At low loading rates (tensile tests conditions) this cavitation/fibrillation process suppresses the crazing of PLA matrix favouring its extensive yielding and plastic shearing.

KEYWORDS: PLA, PLA/PCL, ecoblends, LEFM, fracture behaviour.

1. INTRODUCTION

Poly (lactic acid) (*PLA*) is an interesting and promising bio-based and biodegradable polymer that can be an excellent alternative to petrochemical-based polymers. The applications where *PLA* can be used are vast. From common uses like plastic films and bottles to more complex like biodegradable medical devices.

Certain properties that have restricted its application include low toughness, high gas permeability, reduced temperature resistance and a relatively high cost. In this regard, an important limitation, at least for many marketable applications, is its brittleness. To overcome the inherent brittleness of neat *PLA*, blending with softer polymers has been shown to be one of the most efficient ways to do it.

Yet, unfortunately, the *PLA* blends created present an absence of thermodynamic miscibility with most existing polymers [1]. So, to achieve *PLA*-based blends with good final properties, compatibilization between the blend

components is necessary to be performed. This can be done through the formation of block copolymers and grafting during polymer blending [2].

Various research studies show that the toughness of *PLA* can be improved by blending it with poly (ε-caprolactone) *PCL* [3-8] if good adhesion between both phases is achieved. In a recent work [9] conducted by our group, three *PLA*-based blends using different increasing *PLC* contents (1x, 2x and 3x relative to PLA) with and without an ester-acid based polymeric compatibilizer were produced. According to the morphological analysis and instrumented falling weight impact tests the optimal *PLA/PCL* blend composition was the one with 2x content of *PCL*.

The purpose of this communication is to characterize in deepness the mechanical and fracture behaviour of the optimized *PLA/PCL* blend at moderately high loading rates (1 $m.s^{-1}$).

2. EXPERIMENTAL PROCEDURE

2.1 Materials

The materials used in this study were a PLA ErcrosBio® LL712 (Ercros S.A., Spain) and a *PLA*-ErcrosBio® /*PCL* blend previously prepared using a *PCL* CAPA® 6500 (Ingevity, USA) added in a relative proportion of 2x concerning PLA. As a compatibilizer, it was used an ester-acidic-based copolymer in a proportion of 2y concerning the PCL content in the blend. The details about this compatibilizer and blend composition cannot be provided due to a confidentiality agreement with ERCROS S.A.

2.2 Specimen manufacture

Multipurpose ISO 3167 type 1A test specimens were manufactured using an injection moulding machine Engel Victory 500/100 (GmbH, Germany). Prior to processing, *PLA* and blend were dried at 80 °C for 4h using a dehumidifier hopper (DSN506HE, Piovan S.p.A., Italy) with a dew point of -40 °C. It is worth mentioning that all tests involved in this study were performed after at least 1 week of the specimen manufacturing, when the thermodynamic conditions of typical physical ageing of *PLA* material were equilibrated.

2.3 Tensile properties

They were determined following the ISO 527-2 standard using an universal testing machine Sun 2500 (Galdabini, Italy) equipped with a 1-kN load cell using a crosshead speed of 10 $mm.min^{-1}$. All tests were carried out at room temperature on at least five valid test specimens. The Young's modulus (E), yield strength (σ_y), strain at yield (ε_y), cold drawing stress (σ_{cold}), and strain at break (ε_b) mean values were obtained.

2.4 Impact fracture behaviour

From the central portion of ISO 3167 type 1A specimens, prismatic bars with nominal dimensions of 4 x 10 x 52 mm^3 were cut to meet the dimensional requirements of the single edge notched bend (*SENB*) according to ISO 13586 standard.

Using a manual notching machine (ZwickRoell, GmbH & Co. KG, Ulm, Germany), the *SENB* specimens were V pre-notched in a length to width ratio of 0.45 and a root radius of 0.125 mm. Subsequently, the pre-notches were sharpened through a femtosecond pulsed laser (femtolaser) wich pulses provide rapid thermal ablation (i.e., transforms the material from solid to vapour/plasma) avoiding thermal damage and plastic deformation at the notch tip radius providing a higher quality and close to ideal fissure [10].

Following ISO 17280 standard, the provisional fracture toughness (K_Q) at moderately high loading rates was determined using an instrumented Charpy impact pendulum (CEAST Dartvis, Instron, USA) with an equivalent mass of 3,655 kg an a nominal impact energy of 1,95 J in order to preserve the quasistatic conditions. From reaction force (F_r) vs specimen contact time (t), K_Q was evaluated using equation (1):

$$K_Q = \frac{P_Q}{BW^{1/2}} f \quad (1)$$

Where P_Q is the maximum F_r registered (after a validation procedure according to the standard). B and W *are the* specimen thickness and witdth, respectively. f is a geometric polynomial factor depending on the sharpened notch length (a) to W ratio.

In impact fracture testing, the presence of dynamic effects (inertial loads and vibrations on the test system) produce forces that do not correspond with the forces at the instrumented impact tip of the hammer. In this study, a mechanical damping technique was implemented using a small rubber strip (0.5 mm in thickness) placed in the specimen's portion where the hammer hit. For each specimen tested a fresh strip was used. In this way, the load registered in the load sensor attached to the hammer is the same as the load supported by the specimen and the test can be analyzed as a quasi-static case [11].

In order to obtain a fracture energetic parameter, the impact specific work of fracture (w_f) (i.e., an alternative parameter to the standardized impact resistance) was calculated. In this case, a series of specimens were tested without the damping pad. The total energy consumed (U_{break}) was calculated from *Fr vs. t* traces and w_f was obtained as follows:

$$w_f = U_{break}/S_L \quad (2)$$

Being S_L the ligament section of the specimen.

2.5 Morphological and fractographic studies.

The study was carried out by combining optical microscopy (*OM*) and Scanning Electron Microscopy (*SEM*) (JSM-7001F, JEOL Ltd, Tokyo, Japan) at an acceleration voltage of 2 kV. Previous the analysis was carried out, a thin layer of platinum-palladium at a ratio of 80/20 by weight was deposited on the specimens to be observed.

Two types of fracture surfaces were observed. For the inspection of phases distributions, an untested cryogenic fractured specimen was used. Fractographic analysis was performed on tested broken surfaces. All observations correspond to views perpendicular to the melt flow direction in the mould cavity.

3. RESULTS AND DISCUSSION

3.1 Morphological analysis

It is well known that in blends of immiscible polymers, compatibilized or not, the dispersion and distribution of the phases induced during processing conditions the final performance of the material, and in the rupture stage, the crack propagation features. That is why it is relevant to inspect the morphological characteristics that have been induced during the preparation of the specimens.

Figure 1 shows an image obtained by optical microscopy (*OM*) of a cryogenically fractured surface of the blend. Three different regions can be clearly observed: an elliptical central region (a), an intermediate region that circumscribes the former (b), and one located in the external faces of the specimen (c).

This can be associated with the generation of a morphological gradient as a consequence of the flow pattern formed during the filling of the mould cavity throughout the specimen manufacturing process. *SEM* observations (figure 2) on cryogenically fractured surfaces confirm that depending on the position in the specimen thickness, the dispersed phase (associated with *PCL*) presents different morphologies related to different levels of shear deformation at which the melt is subjected during its advance in the cavity.

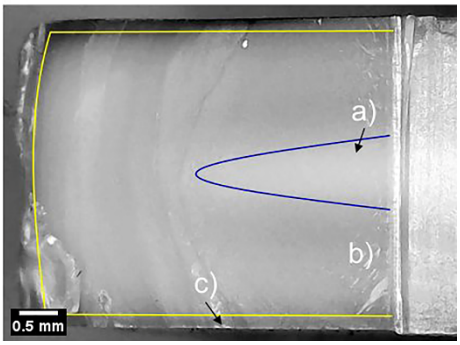

Figure 1. Optical microscopy view of the cryogenic fracture surface.

In figure 2a, it can be seen that at the external faces of the specimen (skin layer, figure 1, region c)) a stratified or layered feature is observed. This is due to that in this region the layer of material takes contact with the cold surface of the mould, freezing and avoiding any brake up/relaxation of the dispersed phase, showing a fiber-like morphology with a high aspect ratio. Successive layers away from this zone will be subjected to lower shearing causing a morphology transition from layers with lower aspect ratio (figure 2b) to a drop-island one (figure 2c), where the shearing deformation has a lower degree.

3.2 Tensile properties

Figure 3 shows representative engineering stress-strain curves for both tested materials. In the blend, a yield point (σ_y) is observed where a geometric softening by necking formation starts. Afterwards, there is a stable neck propagation (cold drawing) where the tensile

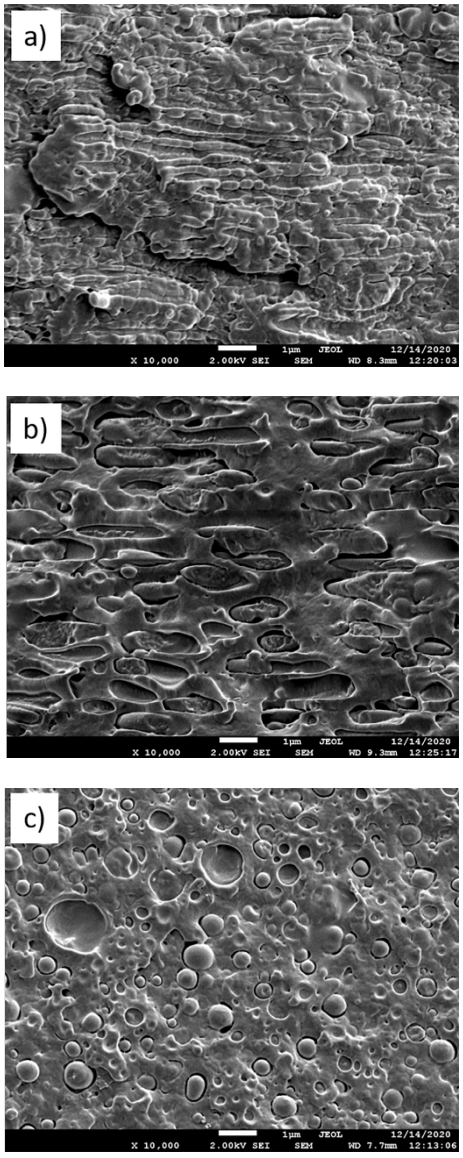

Figure 2. SEM observations of regions a), b) and c) in figure 1.

deformation progressed at a constant stress level (σ_{cold}) until the specimen's rupture.

PLA also showed a yield point at maximum load (σ_y) but, in this case, after this point is reached, a drop in load is accompanied by the break of the specimen in a brittle manner. This was due to the formation of multiple crazes that avoid the propagation of a stable neck [12]. During testing, it was observed that multiple crazing appears at about 0.8 times the σ_y-value observed.

It is worth remembering that the craze formation involves a local yielding of the material, but due to hydrostatic conditions (dictated by the entanglement density of the polymer and its free volume), which avoid an extensive shear yielding lead to the microvoiding structure of craze to be formed.

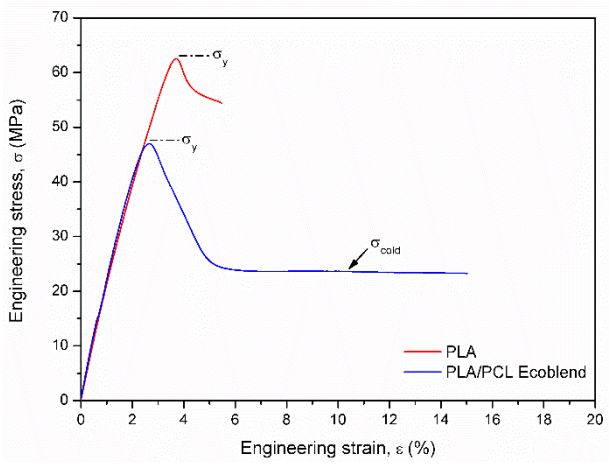

Figure 3. Uniaxial engineering stress-strain curves.

Table 1 collects the main mechanical parameters obtained. It is evident that the addition of *PCL* in the % weight selected and suitable compatibilized doesn't affect the Young's modulus, but produce a decrease of about 25% on the σ_y coinciding roughly with the value where multiple crazing in *PLA* was observed. Additionally, even the high standard deviation obtained for the blends, a clear increase on ε_b (about 165%) is observed.

Table 1. Tensile mechanical properties obtained at 10 mm/min.

Mechanical property	PLA	PLA/PCL Ecoblend
E (GPa)	2.2 ± 0.01	2.5 ± 0.2
σ_y (MPa)	62.2 ± 0.2	46.7 ± 0.4
ε_y (%)	3.80 ± 0.05	2.7 ± 0.1
σ_{cold}	-----	22.3 ± 0.3
ε_b (%)	5.5 ± 0.1	96.0 ± 40.0

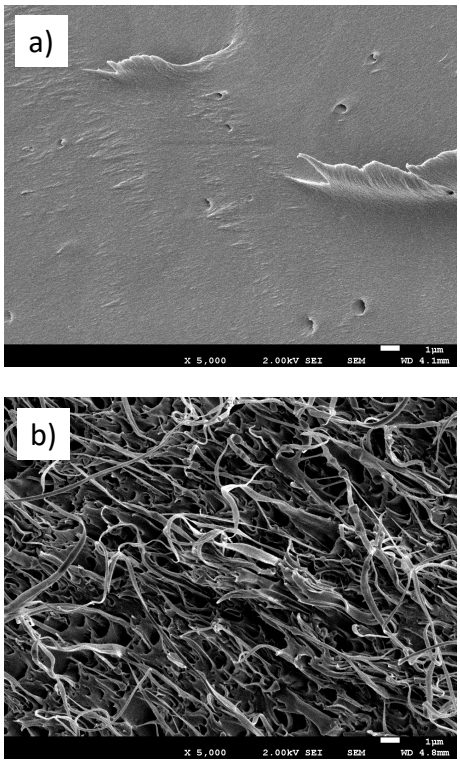

Figure 4. *SEM* observations of fracture surfaces of the central region after tensile testing of a) *PLA* and b) Blend specimens.

Figure 4 shows the fracture surfaces (in the central region) of both materials after tensile testing. As can be seen, while in the *PLA* the generated surface is practically smooth, with little evidence of plastic tearing, in the blend is observed a high degree of tearing together with evidence of fibrillation and even cavitation of the *PCL* phase. This suggests that it is precisely this cavitation that causes a relief of local triaxiality of the *PLA* phase at the moment of its yielding, avoiding the generation of crazes and therefore giving rise an extensive shear yielding of the matrix.

3.3 Fracture behaviour

Figure 5 shows representative reaction force (F_r) vs specimen contact time (t) curves for both materials tested. Dotted curves in figure 5 correspond to tests with an elastomeric layer settled. Independently of the impact mode (with and without damping pad), the force value at fracture initiation remains almost the same, but the fracture time is increased when the elastomeric layer is used.

In these conditions, calculating a fracture energy parameter (G_Q, provisional energy release rate) would deliver an overestimated value. Instead, w_f was evaluated with the procedure explained in Section 2.3.

In table 2 the fracture parameters (K_Q and w_f) obtained are presented. Even those parameters are not in the plane strain condition, they can be used for comparative purposes. As can be seen, the blend shows an increase of

about 65% in K_Q and about 580% in the specific work of fracture in these stress state conditions.

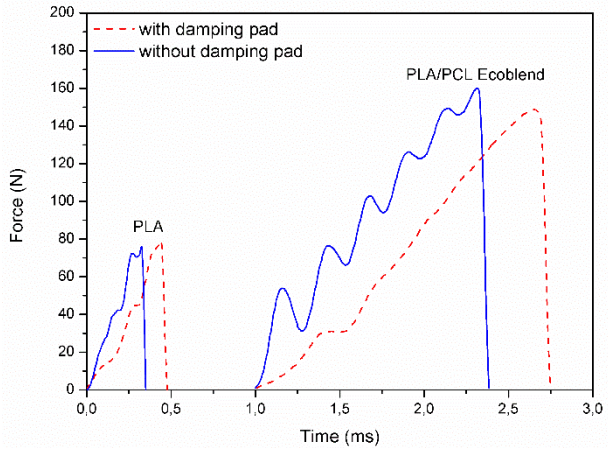

Figure 5. Representative force vs specimen contact time curves at 1 m.s^{-1}) for tested materials.

Table 2. Fracture parameters obtained at moderately high loading rates.

Fracture parameter	PLA	PLA/PCL Ecoblend
K_Q (MPa.m$^{1/2}$)	1.9 ± 0.2	3.2 ± 0.1
w_f (kJ/m^2)	0.8 ± 0.1	5.5 ± 0.6

These trends can be related to the events involved during crack propagation. Evidences which are shown in the *SEM* micrographs of figure 6. For both materials the crack propagates by crazing generation and three distinctive propagation zones could be appreciated: Slow start of crack propagation through the stable rupture of crazes formed (zone 1), the transition from stable to unstable crazing propagation in several planes with the formation of the typical "river pattern" (zone 2), and propagation by the consecutive generation of crazes and decohesion of their fibrils from the region of the active zone of the crazes which altogether forms the also typical "hackle pattern".
It can be seen that the zones of slow propagation (zone 1) and stable-unstable crazing transition (zone 2) are more extensive in the *PLA/PCL* blend. It is also interesting that these zones are replicated towards the final part of the ligament.

In the *PLA/PCL* blend, regions 1 and 2 are characterized by high cavitation of the dispersed phase and sequential fibrillation of the *PLA* matrix, related to the decohesion of the fibrils in the active zone of the crazes and therefore with a slowdown in their formation (figure 7a). In the case of *PLA*, sequential fibrillation is less observable (figure 7b).

As previously mentioned, the cavitation process favors the relief of local triaxiality. Then, to initiate the craze formation and subsequent rupture, a higher local hydrostatic stress must be applied wich also makes the

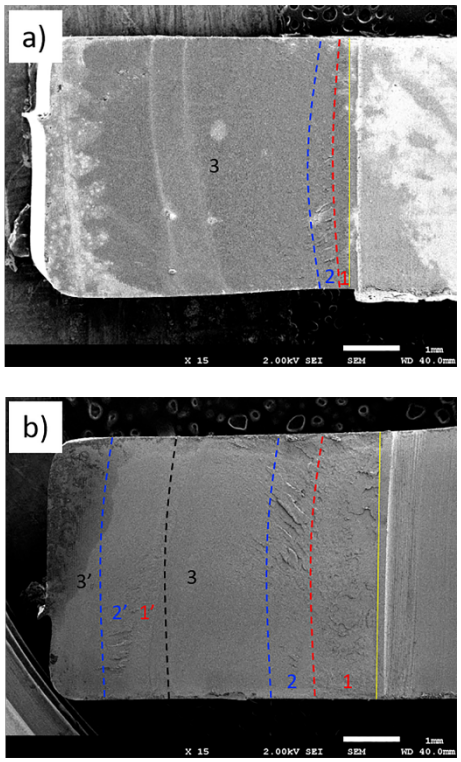

Figure 6. Fracture surfaces showing propagation zones generated during the fracture process: a) *PLA*, b) Blend.

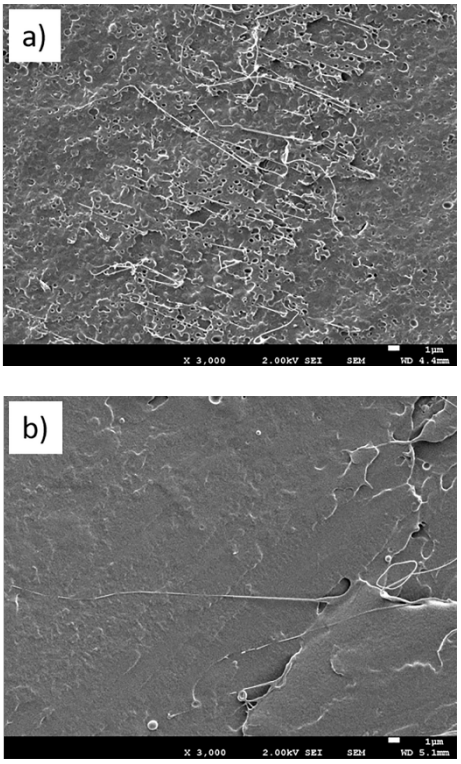

Figure 7. Specific features on the crazing process for propagation zones 1 and 2: a) *PLA/PCL*, b) *PLA*.

fracture toughness (in terms of stress intensification to begin the fracture process) to be greater for the blend (table 2).

Additionally, given the extension of stable zones, replication of fractured regions and the cavitation events involved, makes the energy dissipation greater, delivering an approximate 7x increase for w_f (table 2).

4. CONCLUSIONS

The incorporation of 2x of *PCL* content relative to *PLA* content (as major constituent) promotes an increase of 165% in elongation at break and a reduction of yielding strength of about 25 % without affecting the Young's Modulus.

At moderately high loading rates (impact conditions), *PCL* promotes a 1,5 times increase of stress intensification factor needed to initiate crack propagation, and a 7-time increase of energy consumed during the process.

Fractographic evidences reveals that the *PCL* phase deformation and cavitation promotes a relief of the local triaxiality which can cause an increase of the local hydrostatic stress needed to initiate the crazes and its subsequent rupture in impact conditions. At low loading rates (tensile tests conditions) this cavitation/fibrillation process suppresses the crazing of *PLA* matrix favouring its extensive yielding and plastic shearing.

ACKNOWLEDGEMENTS

The authors would like to thank the Ministry of Science, Innovation and Universities of Spain for the funding received to the project: ECOBLENDS'UP ref PID2019-106518RB-I00.

REFERENCES

[1] Z. Jian-Bing, L. Kun-Ang, D. An-Ke. Compatibilization strategies in poly (lactic acid) – based blends. RSC Adv (2015) 5: 32546-32565. https://doi.org/10.1039/c5ra01655j.

[2] X. Zhao, H. Hu, X. Wang, X. Yu, W. Zhou, S. Peng. Super tough poly (lactic acid) blends: a comprehensive review. RSC Adv (2020) 10: 13316-13368. https://doi.org/DORAO1801E.

[3] A. Ujcic, I. Fortelny, S. Krejcikova, E. Pavlova, J. Hodan, M. Slouf. Effects of thermal treatment and nucleatings agents on crystallinity, toughness, and stiffness of PLA/PCL blends. Express Polym Lett (2022) 16: 221-233. https: //doi.org/ 10.3144/ expresspolymlett.2022.18.

[4] I. Fortelny, A. Ujcic, L. Fambri, M. Slouf. Phase structure, compatibility and toughness of PLA/PCL blends: A review. Front Mater (2019) 6: 206. https://doi.org/10.3389/fmats.2019.00206.

[5] M. Delgado-Aguilar, R. Puig, Ll. Sazdovski, P. Fullana-i-Palmer. Polylactic Acid/Polycaprolactone blends: On the path to circular economy, substituting single-use commodity plastics products. Materials (2020) 13: 2655. https: //doi.org /10.3390/ma13112655.

[6] T. Takayama, M. Todo, H. Tsuji. Effect of annealing on the mechanical properties of PLA/PCL and PLA/PCL/LTI polymer blends. J Mech Behav Biomed Mater (2011) 4: 255-260. https: //doi.org/10.1016/j.jmbbm.2010.10.003.

[7] A.K. Matta, R. Umamaheswara Rao, K.N.S Suman, V. Rambabu. Preparation and characterization of biodegradable PLA/PCL polymeric blends. Procedia Mater Sci (2014) 6: 1266-1270. https: //doi.org/10.1016/j.mspro.2014.07.201.

[8] H. Zhao, G, Zhao. Mechanical and thermal properties of conventional and microcellular injection molded poly (lactic acid)/poly (ε-caprolactone) blends. J Mech Behav Biomed Mater (2016) 53: 59-67. https://doi.org/10.1016/ j.jmbbm.2015.08.002.

[9] N. León, T. Abt, M. Hórtos, S. Espino, O.O. Santana, M. Ll. Maspoch. Impact behaviour of PLA/PCL bioblends. 37 Congreso del Grupo Español de Fractura – 1st Virtual Iberian Conference on Estructural Integrity (2020) 182-187.

[10] N. León, A.B. Martínez, P. Castejón, D. Arencón, P.P. Martínez. The fracture testing of ductile polymer films: Effect of specimen notching. Polym Test (2017) 63: 180-193. http: //dx.doi.org/ 1016/j.polymertesting.2017.05.022.

[11] N. León, A.B. Martínez, M. Maspoch. Notch effect on the linear elastic fracture mechanics values of a polysulfone thermoplastic polymer. Theor Appl Fract Mech (2021) 114: 102995. https://doi.org/ 10.1016/j.tafmec.2021.102995.

[12] J. Cailloux, O.O. Santana, E. Franco-Urquiza, J.J. Bou, F. Carrasco, M. Ll. Maspoch. Sheets of branched poly(lactic acid) obtained by one-step reactive extrusión-calendering process: physical aging and fracture behavior. J. Mater. Sci. (2014) 49: 4093-4107. https://doi.org/10.1007/s10853-014-8101-y.